processes

MDPI

Article

Research of an Abandoned Tailings Deposit in the Iberian Pyritic Belt: Characterization and Gross Reserves Estimation

Diego Davoise [1,2,*] and Ana Méndez [1]

[1] Department of Geological and Mining Engineering, Mines and Energy School, Universidad Politécnica de Madrid, 28040 Madrid, Spain; anamaria.mendez@upm.es
[2] Atalaya Riotinto Minera SLU, La Dehesa S/N, 21660 Minas de Riotinto, Spain
* Correspondence: dp.davoise@alumnos.upm.es

Abstract: Global situations such as economic recovery after a pandemic, geopolitical instability, and future digital and energy transition are some of the drivers for the European Union (EU) to explore new and existing sources of raw materials. The Iberian Pyrite Belt in the southwest of the Iberian Peninsula (Spain and Portugal) hosts a great number of tailing deposits from centuries of mining operations. A unique tailings deposit has been studied and characterized. The similarities with other tailing deposits deeply studied suggested the presence of critical raw materials. Furthermore, a very gross reserves estimation was made. The characterization and reserves estimations were compared with the bibliography from mining companies who operated in the area decades ago and from the bibliography available at Fundación Riotinto. The presence of critical raw materials was confirmed, some of them in high concentrations. Moreover, a singular difference was found compared with other similar tailings stored within the Iberian Pyrite Belt. The main valuable metals identified were Au (2.25 ppm), Ag (215 ppm), Co (131 ppm) and Cu (0.29%). The reserves estimation showed that this deposit potentially hosts 1.86 t of Au, 177 t of Ag, 108 t of Co or 2358 t of Cu; in other words, with a copper average price of 8366 US$/t in December 2022, the tailings deposit contains a potential value of more than 19 million USD.

Keywords: secondary raw materials; critical raw materials; abandoned tailings deposit

Citation: Davoise, D.; Méndez, A. Research of an Abandoned Tailings Deposit in the Iberian Pyritic Belt: Characterization and Gross Reserves Estimation. *Processes* **2023**, *11*, 1642. https://doi.org/10.3390/pr11061642

Academic Editor: Guining Lu

Received: 29 April 2023
Revised: 25 May 2023
Accepted: 25 May 2023
Published: 27 May 2023

1. Introduction

The current energetic model and the increasingly technology-based economy are two of the main drivers for demand increase for mineral resources, especially those known as base and critical metals [1]. Countries with an extensive need for materials for their social and economic development are playing a key role in global demand for resources.

Often, these raw materials are technically and economically challenging to obtain from primary deposits. Moreover, primary deposits with high grades are becoming depleted, so new orebodies with lower grades and high complexity appear to be the new future for the mining industry [2]. The appetence for raw materials thus cannot be satisfied without understanding the social and environmental consequences it has. In 1987, the report "Our Common Future" by the World Commission on Environment and Development defined sustainable development as a "development that meets the needs of the present without compromising the ability of future generations to meet their own needs" (in other words, ensuring their inter-generational equity) [3]. Historically, mining activities have been linear processes; however, nowadays, a shift is required toward a more circular management of mineral resources.

To reduce the import imbalance and increase its self-sustainability, it is a priority for the EU to find new sustainable and affordable secondary supply sources within the European borders. During 2011, the EU issued the first list of critical raw materials, which has been updated four times since then. This list highlights those raw materials considered

strategic for the European economy but also those at high risk of availability or supply [1]. Existing tailing dams along the EU are nowadays under the spotlight due to containing both categories of raw material, secondary and critical raw materials.

The role of mine wastes in the sustainable supply of raw materials has yet to be evaluated in depth. There are four types of mine waste deposits with high potential: (1) mine dumps with discarded by-products from the past mining of other minerals that now are considered critical; (2) mine dumps containing minerals in which present technologies have reduced the cut-off grade, making lower grade ores now profitable; (3) mine tailings with elements that were not previously identified or recovered with conventional separation techniques [4]; (4) tailings from extraction plants not properly scaled to the ore grade of the input, producing low recovery factors. The mineral resources in these deposits can have massive scales, particularly in open pit mines where the rate between ore and the by-product is very low.

Mine waste deposits thus represent a very suitable secondary source of mineral resources. The lower costs in terms of energy, resources and risk compared to primary extraction operations make it reasonable to explore the potential of materials that have been already unearthed [5,6]. In addition, the mineral extraction from mine waste is not only economically profitable but can also restore degraded landscapes and in many cases can mitigate or remove uncontrolled sources of acid or metal-rich drainages [7].

In relation to this, the Iberian Pyrite Belt, in the southwest of the Iberian Peninsula, hosts some of the oldest mines in the world [8]. It is known that original Riotinto mine was already mined during Roman times, being gold and silver two of the metals extracted at that time. More mining operations have taken place within the Iberian Pyrite Belt since then; consequently, the number of tailing deposits is also increasing.

Tailings and residues from mining and metallurgical processes used to be mainly stored in waste rock dumps and/or tailing deposits. Tailings characteristics vary depending on the ore mined and the treatment applied to the ore. Waste rock dumps often host material extracted from the mine. This material corresponds to pure gangue, low-grade ores or simply complex ores difficult to treat with available technologies. On the other hand, tailing deposits store material rejected during the separation/concentration treatment of the mineral of interest. Generally, tailings are fine grain size materials; the reason lies in the fact that minerals have to be finely grinded in order to be liberated and concentrated later on. For years, the Iberian Pyrite Belt was one of the largest sources of pyrite for sulfuric acid production [8]. Morrongos was the name given to the residues generated after open-air pyrite roasting [9]. In some cases, Morrongos were processed again with the objective of extracting the remaining fresh pyrite or its copper-bearing minerals [8,10].

The Iberian Pyrite Belt is one of the most widely studied areas with regard to geology and mining. Many researchers have studied the variety of tailing deposits, especially in the Riotinto district [11–15] and those related to residues from open-air pyrite roasting [16,17].

The main objective pursued by this study is to perform a wide characterization of a unique abandoned tailings deposit located in the southwest of Spain. The similarities with other waste deposits storing residues from open-air pyrite roasting suggests the presence of critical raw materials. In addition, a very gross reserves estimation was made in order to assess its potential as a secondary resource of raw materials or critical raw materials. The characterization and reserves estimation were compared with the bibliography from mining companies who operated in the area decades ago and from the bibliography available at Fundación Riotinto.

2. Materials and Methods

2.1. Sample Selection

The studied abandoned deposit is located within the Pyrite Belt in Minas de Riotinto (Figures 1 and 2), Huelva (Spain). It is known as "Zarandas", its reference ID for the Instituto Geológico y Minero de España (Table 1) national tailing deposit database is 0938-8-0002 [18].

Figure 1. Tailings deposit location at Minas de Riotinto, Huelva province (Spain) [source: own elaboration].

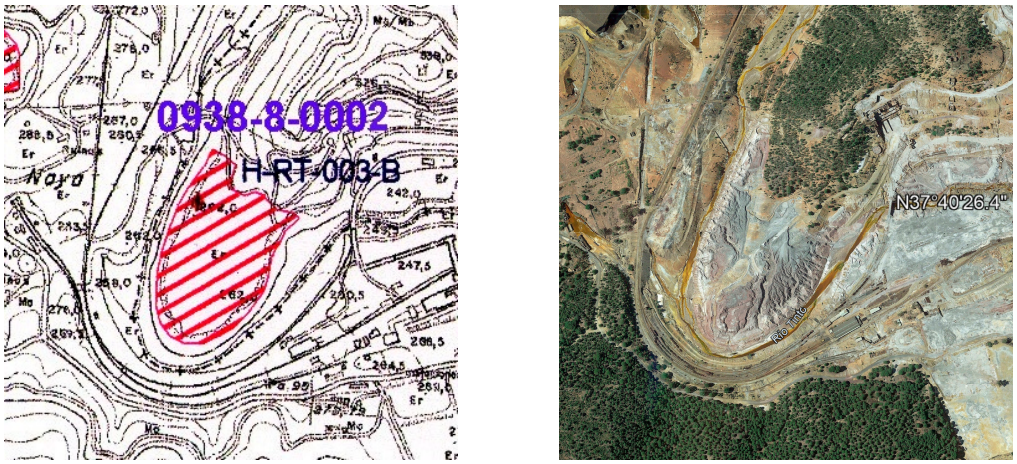

(**a**) (**b**)

Figure 2. Tailings deposit location. (**a**) Identification number established by the Instituto Geológico y Minero de España (IGME), 0938-8-0002 [18]; (**b**) Orthophoto of the tailings deposit [picture downloaded from Google Earth].

Table 1. Tailings deposit identification and coordinates by Instituto Geológico y Minero de España [18].

		ETRS89		
Name	**ID**	**Latitude**	**Longitude**	**Coordinate Z**
Zarandas	0938-8-0002	−6.559775509295264	37.67314575524642	262

This deposit hosts a mix of fine material rejected from a washing plant which treated residues from open-air pyrite roasting, low copper content pyrites and chlorites [8,10]. The plant aimed to wash these materials in order to obtain a concentrate of pyrites under specific parameters, for instance: sulfur grade (>48%) and materials with a particle size between 1/2 and 1/4 inches [8,10]. The plant was a combination of three concentration stages, medium dense separators, Wilfley shaking tables and flotation cells. The fines and ultra-fines were considered waste, as there was no market for them.

2.2. Sampling and Preparation

A sample of 2 kg was collected. Surface samples were gathered from a single spot with a shovel and stored in a propylene bag in 2020. The sample was sieved at 2 mm, homogenized manually (Figure 3), and aliquot samples were taken for its chemical, mineralogical and physical analysis.

(**a**) (**b**)

Figure 3. Sample preparation. (**a**) Sample "as found" [own elaboration]; (**b**) Sample sieved and homogenized [own elaboration].

2.3. Sample Characterization

2.3.1. Chemical Analysis

For the solid sample, wavelength X-ray fluorescence (WDXRF) was performed in an ARL ADVANT'XP + sequential model from THERMO (SCAI-Málaga University, Málaga, Spain). Concentration data were obtained using the UNIQUANT Integrated Software. The chemical composition was complemented for trace elements by ALS Laboratory group and Atalaya Mining Laboratory. Base metals were determined inductively by coupled plasma optical emission spectrometry (ICP Avio 500, Perkin Elmer Inc., Waltham, MA, USA) (ICP-OES) with A33 and IT-LAB-28 protocols, a multi-acid digestion procedure with HCl, HNO_3, HF and $HClO_4$, and an acid digestion with HNO_3 and HCl, respectively. Rare earth elements were determined by the ME-MS81 ALS procedure, PGM following the PGM-ICP23 protocol, and gold was determined by a 30 g FA ICP.

2.3.2. Mineralogical Analysis

Mineralogical characterization was examined by three techniques. The first mineralogical test was completed with a CAMEVA system [19,20]. The test was carried out at the Laboratory of Applied Microscopy (LMA, Universidad Politécnica de Madrid, Madrid, Spain). CAMEVA is a multispectral reflectance microscopy system conceived to identify and characterize the mineral phases present in a sample; this system is able to identify minerals from their multispectral signature in the visible and near-infrared range between 400 and 1000 nm.

The second technique employed was XRD using the Minerals Edition of Aeris compact X-ray diffractometer (Malvern Panalytical B.V., Almelo, The Netherlands) (40 kV–15 mA), with a goniometer radius of 145mm, Kα = 1.79 Å cobalt-anode X-ray tube, 0.04 Soller slits, 1/4 divergence slits, 23 mm mask, low beam-knife, step size 0.02° and acquisition time of 80 s/step. [21]. For XRD analysis, the sample particle size was already below 50 µm, so no further milling was required in order to improve mineral quantification. The sample was prepared in a 27mm backloading sample holder to reduce preferential orientation.

Finally, the mineralogical study was concluded with SEM-EDS analysis and carried out by the Centro de Investigación en Química Sostenible (CIQSO) at Huelva University. It was performed using a JEOL JSM-IT 500 HR microscope fitted with an Oxford X-Max 150 field emission source for SEM.

2.3.3. Further Chemical and Physical Characterization

Four particle size distribution measures were taken by a laser diffractometer, the Mastersizer 3000E (Malvern Panalytical, Malvern, UK). The final result is an average of the four measures.

The composition and paragenesis of copper-bearing minerals are very complex and varying. There is a range of tests that can be performed to differentiate the valencies of copper in a copper-bearing ore, in other words, the mineralogical forms of copper in the ore [22].

A sequential copper test designed by METCON Research Inc. [23] was performed in order to estimate the distribution of copper minerals in the sample as a function of the total copper present in the ore. The test follows three stages. Firstly, the sample is leached with sulfuric acid (5%), and the metal extracted is considered acid-soluble oxidized copper compounds. Second, the residue is leached with sodium cyanide (10%), so the metal extracted corresponds to non-refractory copper minerals or secondary copper sulfides. Third, the final residue is digested with three acids, HCl, HNO_3 and $HClO_4$ and analyzed. The copper reported is defined as refractory copper mineral or primary copper sulfide (chalcopyrite).

A 50 mL pycnometer was used to determine the specific gravity. In addition, natural pH and Eh were measured using a Crison micro pH 2000 and Eh in a pH 60 DHS, respectively, after stirring for 1 h in distilled water (0.25 mL) with a sample (0.1 g) using a thermostatic bath with stirring.

2.4. Tailings Deposit Volume Estimation

The tailings deposit volume was calculated with Global Mapper software. The volume was estimated overlapping two Digital Terrain Models, the "original terrain" (Figure 4) and present terrain (Figure 5), so the fill volume was calculated. In order to create the original terrain model, an old paper plan [24] was scanned, digitalized and georeferenced with AutoCAD Civil 3D; the level curves and surface model were created with Global Mapper (Figure 4).

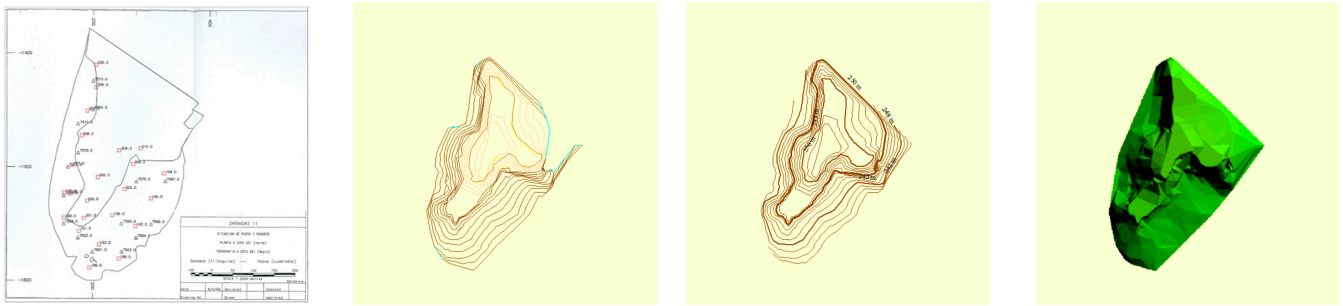

(**a**) (**b**) (**c**) (**d**)

Figure 4. Process to create a Digital Model Terrain (Original Terrain) from a paper plan. (**a**) Scanned original plan [24]; (**b**) Plan digitalized by AutoCAD Civil 3D [own elaboration]; (**c**) Curve model drawn with Global Mapper [own elaboration]; (**d**) Final DTM from scanned plan [own elaboration].

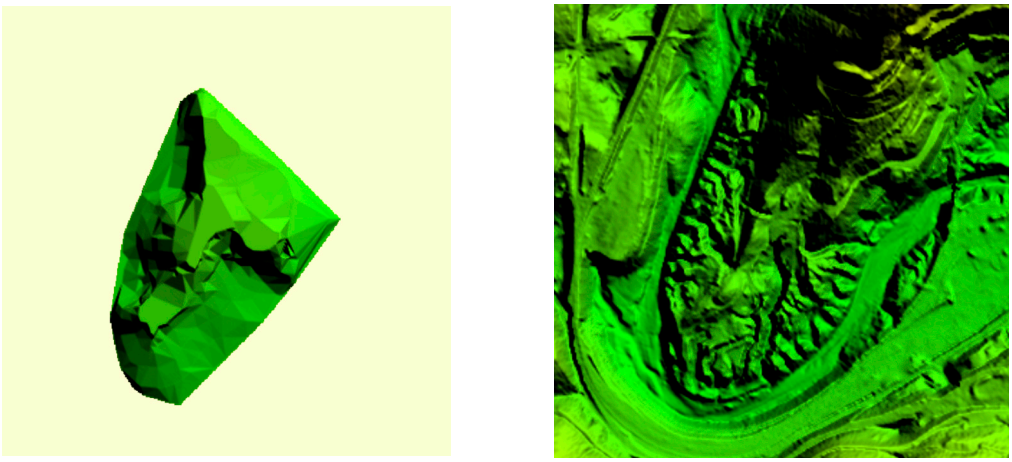

(**a**) (**b**)

Figure 5. DTM used for volume estimation. (**a**) Original terrain [own elaboration]; (**b**) Latest DTM available at Instituto Geográfico Nacional (derivated work from MDT02 2019 CC-BY 4.0 scne.es) [25].

The latest DTM available, MDT02 (2015-Date), at the National Institute of Geography of Spain (Instituto Geográfico Nacional) was downloaded as the present terrain. The features of the latest DTM are shown in Table 2.

Table 2. Latest DTM file features available at Instituto Geográfico Nacional (MDT02 2019 CC-BY 4.0 scne.es) [26]. Flight 2015–2021.

Features	Second Flight
Density	0.5–2.0 p/m^2
Geodetic system	ETRS89 zones 28–31
Altimetric system	Orthometric heights, reference geoid EGM08
RMSE Z	$\leq$20 cm
Estimated planimetric accuracy	$\leq$30 cm
Simultaneous picture	Yes, since 2016
Document size	2 × 2 km (exception Madrid)
Document format	LAS 1.2 format 3
MDE	2 m × 2 m
RMSE Z (MDE)	$\leq$25 cm
Estimated planimetric accuracy (MDE)	$\leq$50 cm

This volume estimation is compared with previous estimations carried out by two mining companies which operated in the area between 1999 and 2014.

3. Results

3.1. Compounds and Elements Present in the Sample

Compounds and elements analyzed by X-Ray Fluorescence (XRF) are reported in Table 3. The principal elements present in the sample were Fe (20.38 wt%), Si (7.31 wt%), S (5.00 wt%), As (2.30 wt%), Al (2.18 wt%) Pb (2.08 wt%) and Ca (1.01 wt%). Base metals such as Ag (215 ppm) and Cu (0.29 wt%) and critical raw materials such as Sb (2700 ppm), Bi (425 ppm) and Co (131 ppm) were identified by XRF as well.

Table 3. X-Ray fluorescence analysis [own elaboration].

Major Compounds (wt%)										
Fe_2O_3	**SiO_2**	**Al_2O_3**	**CaO**	**PbO**	**K_2O**	**SO_3**	**TiO_2**	**As_2O_3**	**Sb_2O_3**	**BaO**
29.14	15.64	12.5	4.12	3.04	3.04	2.24	0.76	0.71	0.36	0.32
ZnO	**CuO**	**SnO_2**	**MgO**	**Ag_2O**	**P_2O_5**	**Bi_2O_3**	**ZrO_2**	**Co_3O_4**		
0.32	0.26	0.24	0.09	0.07	0.05	0.02	0.02	0.02		
Major elements (wt%)										
Fe	**Si**	**Sx**	**As**	**Al**	**Pb**	**Ca**	**Ba**	**K**	**Cu**	**Sb**
20.38	7.31	5.00	2.30	2.18	2.08	1.01	0.64	0.63	0.29	0.27
Minor elements (ppm)										
Sn	**Ti**	**Zn**	**Bi**	**Mg**	**Px**	**Ag**	**Zr**	**Co**	**Hg**	**Se**
0.20	0.19	0.19	425	413	377	215	148	131	102	80

Chemical analyses with ICP-OES (A33 and IT-LAB-28 protocols) are shown in Table 4. The major elements identified were Fe (25.26 wt%), S (12.76 wt%), As (2.97 wt%), Pb (2.59 wt%), Al (1.92 wt%) and Ca (1.11 wt%). Base metals such as Cu (0.29 wt%) and Zn (0.20 wt%) or Ag (199 ppm) were present in lower concentrations. Critical raw materials were present too, such as Sb (0.15 wt%), Bi (348 ppm) and Co (35 ppm).

Table 4. ICP-OES analysis [own elaboration].

Major Elements (wt%)										
Fe	**S**	**As**	**Pb**	**Al**	**Ca**	**K**	**Cu**	**Zn**	**Sb**	**Ti**
25.26	12.72	2.97	2.59	1.92	1.11	0.62	0.29	0.20	0.15	0.12
Minor elements (ppm)										
Sn	**Mg**	**Bi**	**Ba**	**Ag**	**Hg**	**Zr**	**Sr**	**Co**		
805	742	348	269	199	117	110	49	35		

Analysis for REE, PGM and Au are reported in Table 5. REEs were present in the sample), as well as Au (2 ppm), while PGMs were reported in lower concentrations, such as Pt (0.008 ppm) and Pd (0.003 ppm)

Table 5. Content of minor elements including Au, REE and PGM [own elaboration].

Minor Elements (ppm)										
Ba	**Sn**	**Sr**	**Ce**	**V**	**Rb**	**La**	**Y**	**Cr**	**Nd**	**Ga**
4030	1265	54	44	41	39	26	21	20	18	9
Nb	**W**	**Th**	**U**	**Pr**	**Hf**	**Dy**	**Sm**	**Gd**	**Yb**	**Er**
9	8	7	5	5	5	3	3	3	3	2
Au	**Cs**	**Eu**	**Ho**	**Ta**	**Tb**	**Tm**	**Lu**	**Pt**	**Pd**	**TRRE**
2	2	0.8	0.73	0.7	0.52	0.37	0.35	0.008	0.003	130.37

3.2. Mineralogical Composition

The results obtained by the CAMEVA system indicated the presence of pyrite (27.98 wt%), hematite (15.35 wt%), minio (4.65 wt%) and enargite (0.14 wt%). Four major mineral phases were identified by XRD, pyrite, quartz, muscovite and gypsum. SEM-EDS reported an inequigranular distribution with particles from 200 to 0.1 µm, while the main minerals identified were silicates and iron oxides (Figure 6). Moreover, Ca+Fe sulfates and pyrite were reported. The presence of Pb was mainly associated to O+S, while Cu+Zn+Ti had minor concentrations (Figure 7). The mineralogical results are summarized in Table 6.

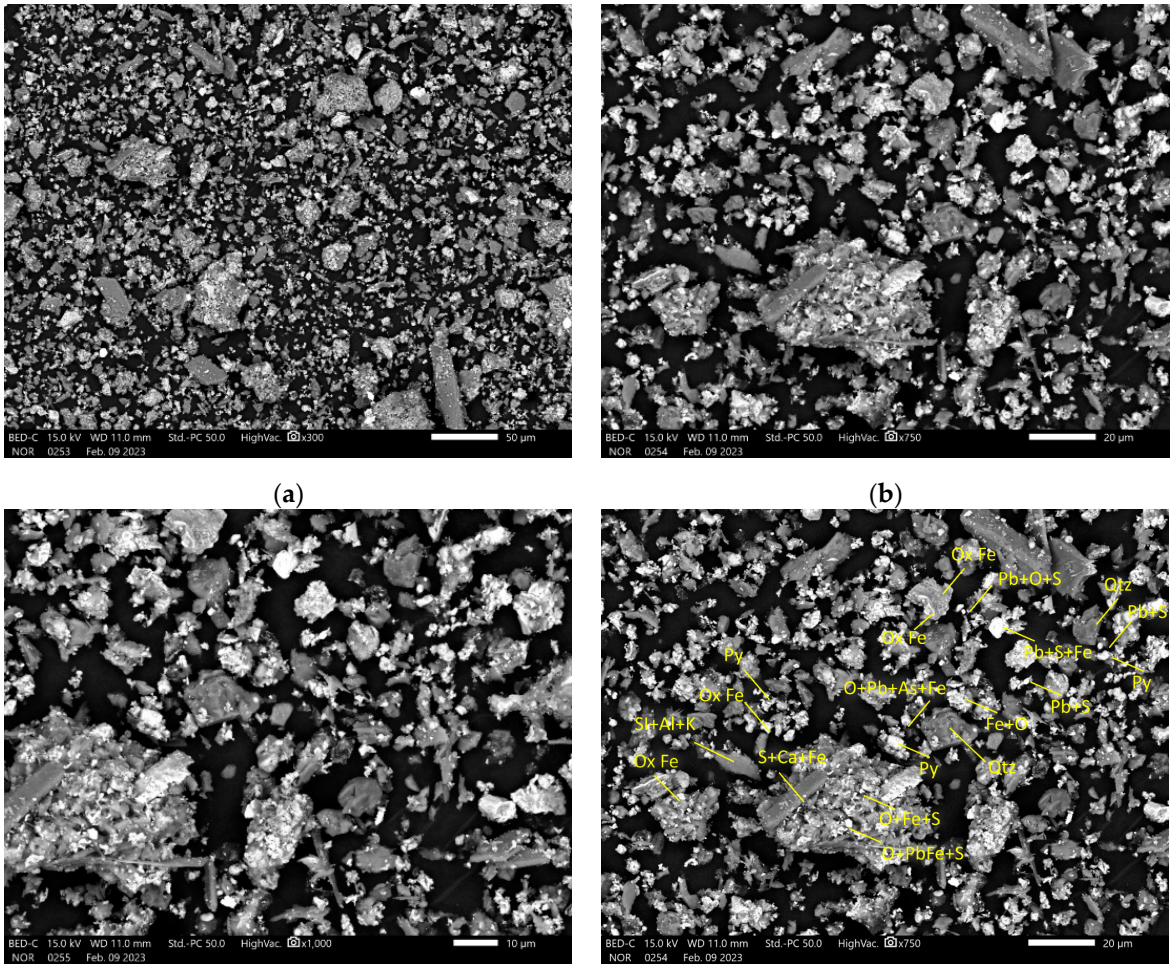

Figure 6. Micrographs obtained by SEM-EDS [micrographs provided by Centro de Investigación en Química Sostenible, Huelva University]. (**a**) Micrograph at 50 µm; (**b**) Micrograph at 20 µm; (**c**) Micrograph at 10 µm; (**d**) Micrograph at 20 µm with species identification.

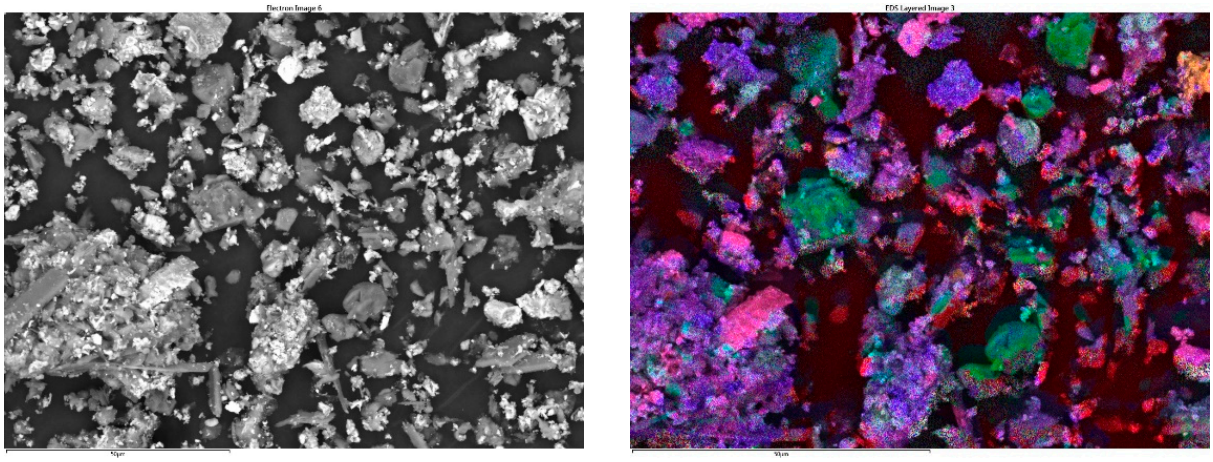

Figure 7. *Cont.*

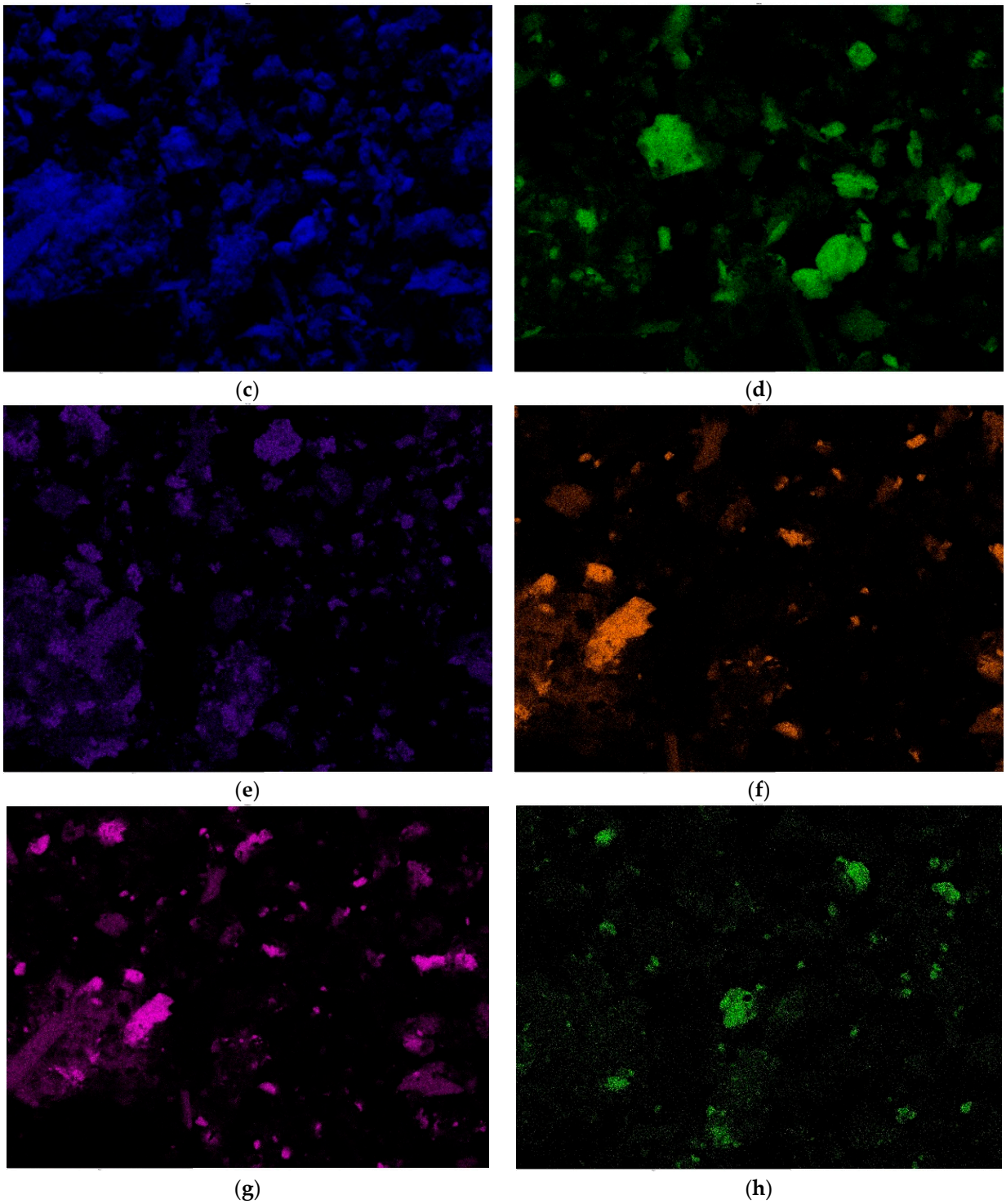

(**c**) (**d**)

(**e**) (**f**)

(**g**) (**h**)

Figure 7. *Cont.*

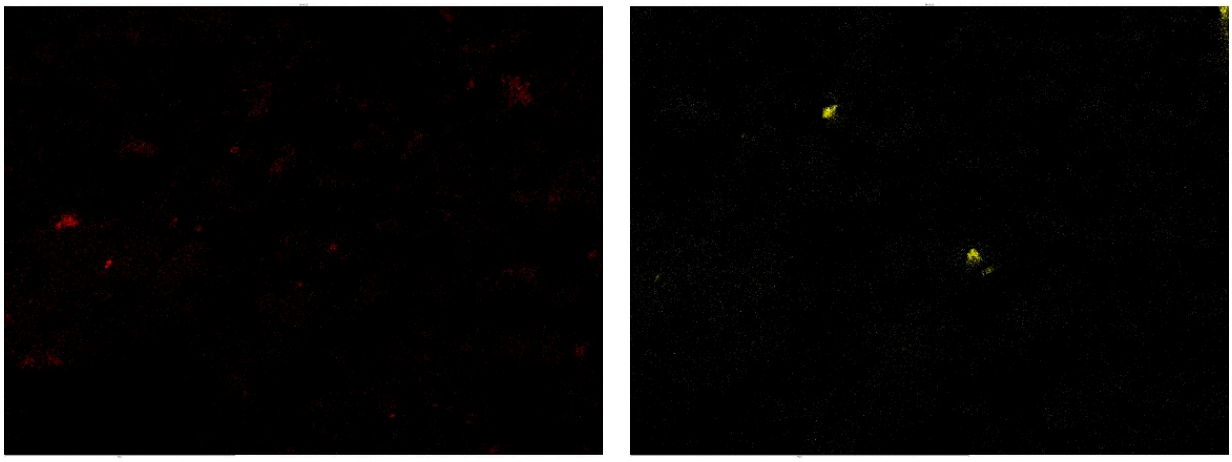

(**i**) (**j**)

Figure 7. X-Ray elements map [images provided by Centro de Investigación en Química Sostenible, Huelva University]. (**a**) Micrograph at 10 µm; (**b**) Multielement X-ray map; (**c**) O map; (**d**) Si map; (**e**) Fe map; (**f**) S map; (**g**) Pb map; (**h**) As map; (**i**) Cu map; (**j**) Zn map.

Table 6. Mineralogical composition of the sample performed by CAMEVA, XRD and SEM-EDS [own elaboration].

Technique	Mineralogy
CAMEVA	Pyrite, hematite, minio *, enargite
XRD	Pyrite, quartz, muscovite, gypsum
SEM-EDS	Pyrite, quartz, iron oxides, calcium and iron sulphates

* Minio is a lead-bearing mineral, it is considered a fairly unusual mineral. Its color is red and in the past, it was widely used as pigment.

3.3. Particle Size Distribution Sample

SEM-EDS analysis reported the presence of a fine material range from 0.1 to 200 µm (Figure 6c). The particle size distribution was measured 4 times (Figure 8) with a laser diffractometer; the average of the results is represented in Table 7. The D_{50} and D_{80} reported were 1.93 µm and 23.53 µm, respectively.

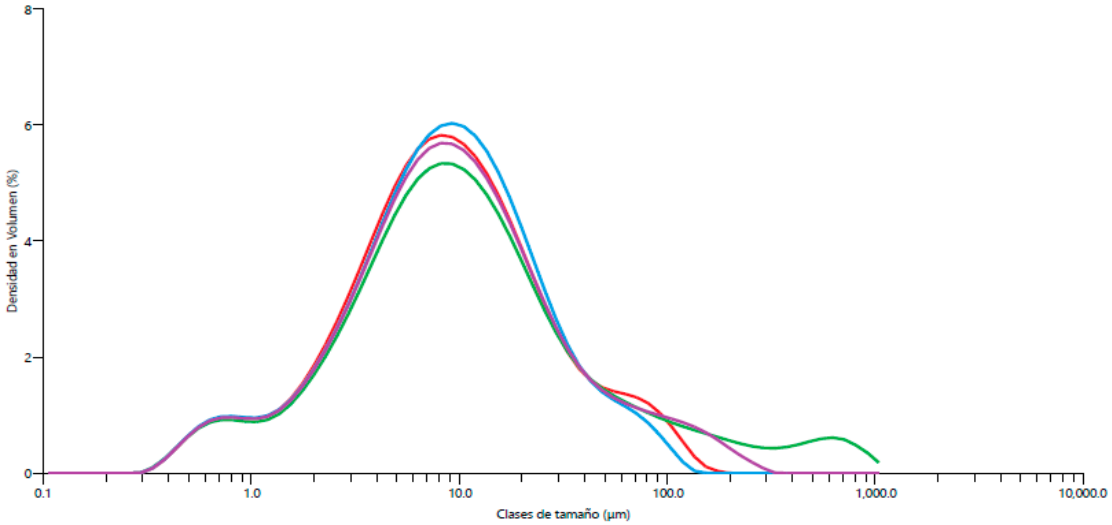

Figure 8. Particle size distribution graph [own elaboration].

Table 7. Particle size distribution results and average [own elaboration].

Test	D_{10} (µm)	D_{50} (µm)	D_{80} (µm)	D_{90} (µm)	D_{100} (µm)
#1	1.91	8.49	21.10	37.90	182.00
#2	1.99	9.61	29.70	80.00	1110.00
#3	1.90	8.64	20.10	32.30	140.00
#4	1.92	8.89	23.20	45.60	307.00
Average	1.93	8.91	23.53	48.95	432.25

3.4. Sequential Copper, Specific Gravity, Natural pH and Eh

Table 8 shows the results from sequential copper test, specific gravity, natural pH and Eh.

Table 8. Copper distribution, specific gravity, natural pH and Eh [own elaboration].

Sequential Copper			
Copper Distribution	**Leaching Agent**	**Concentration (ppm)**	**Distribution (%)**
Oxidized copper	H_2SO_4	2056	78.5
Secondary copper sulfide	NaCN	334	12.8
Primary copper sulfide	Unleached copper	227	8.7
Total		2617	100
Specific gravity	**pH**	**Eh (mV)**	
2.97	2.04	665	

3.5. Tailings Deposit Volume

The Zarandas tailings deposit has been studied by different mining companies over the years [24,27]. Volume estimation is key for reserves estimation; three different approaches are presented in this article. The volume and tons estimated are shown in Table 9. A density of 1.86 g/cm^3 was used to calculate the tons of tailings deposited.

Table 9. Volume and tons estimations (1999–2022) [own elaboration].

Company	Date	Software	Status	Volume (m^3)	Tons
MRT SAL	1999	Datamine	Before mining activities	586,689	1,091,241
EMED Mining	2014	Surpac		582,125	1,082,753
MRT SAL	2002	Datamine	After mining activities	343,239	638,425
Present study	2022	Global Mapper		443,340	824,612

3.6. Reserves Estimation

3.6.1. Present Reserves Estimation

A gross reserves estimation using the tons and the sample XRF analysis for Fe and Cu, ICP-OES for Ag, Sb and Co, and ICP for Pd, Pt and Au has been made during the present study. The reserves are reported in Table 10.

Table 10. Reserves estimation 2022 [own elaboration].

Total			**kg**			**Tons**				
Volume	**Tons**	**Analysis**	**Pd**	**Pt**	**Au**	**Co**	**Ag**	**Sb**	**Cu**	**Fe**
443,340	824,612	XRF	-	-	-	108	177	2193	2358	168,056
		ICP-OES	-	-	-	29	164	1237	2358	216,543
		ICP	2.47	6.60	1.86	-	-	-	-	-

3.6.2. Reserves Estimation Comparison

A comparison between reserves estimation worked out in 2002 and 2022 is shown in Table 11.

Table 11. Comparison between 2002 and 2022 [own elaboration].

			Metals (t)					
Company	**Date**	**Total (t)**	**Au**	**Ag**	**Zn**	**Cu**	**S**	**Pb**
MRT SAL	2002	638,425	0.87	58	945	2552	174,215	11,053
Present study	2022	824,612	1.86	177	1567	2358	41,231	17,152

3.7. Tailings Deposit Aging

Along the years, we observed a change in the deposit landscape due to its physical–chemical properties as well as for weathering. Landscape changes are shown in the orthophoto sequence from 1956 to the present (Figure 9) [25]. It is also represented by the DTM generated and used during the present study (Figure 10).

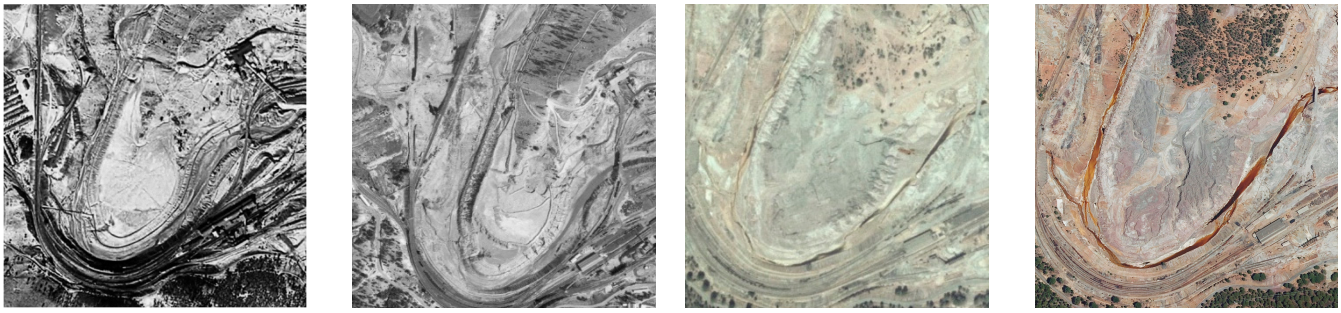

(**a**) (**b**) (**c**) (**d**)

Figure 9. Aging from 1956 to present [25]. (**a**) Orthophoto AMS 1956–1957 (CC-BY 4.0 scne.es 1956–1957); (**b**) Interministerial flight 1973–1986 (CC-BY 4.0 scne.es 1976–1986); (**c**) Quinquennial flight 1998–2003 (CC-BY 4.0 scne.es 1997–2003); (**d**) PNOA Orthophoto (CC-BY 4.0 scne.es 2021).

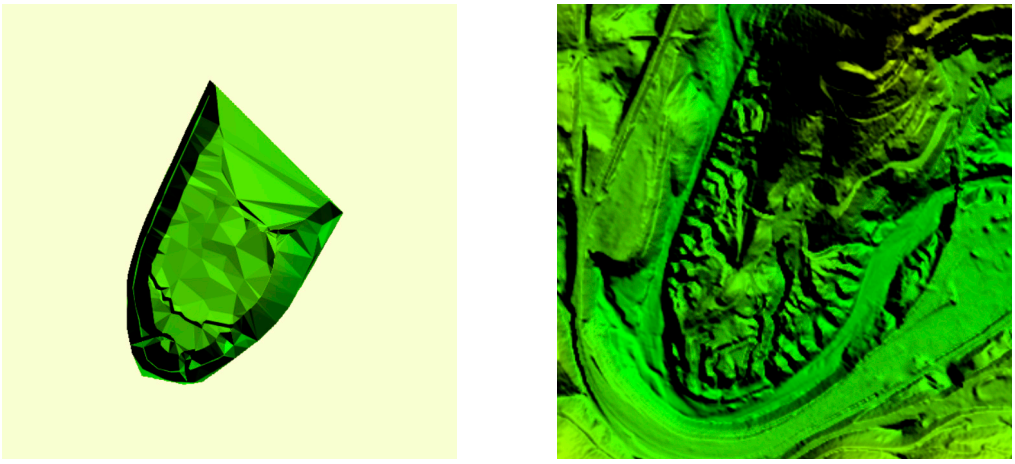

(**a**) (**b**)

Figure 10. The DTM for comparison purposes. (**a**) DTM of original tailings deposit morphology [own elaboration]; (**b**) Latest DTM (MDS02) available at Instituto Geográfico Nacional (derivated work from MDT02 2019 CC-BY 4.0 scne.es) [28].

4. Discussion

The Zarandas tailings deposit hosts the rejected material from a nearby old washing plant.

Base metals (Cu, Zn and Pb) were identified as well as critical raw materials (REE, PGM, Sb, Co and Bi) and precious metals (Au and Ag). These metals and critical raw materials account for more than 20,000 t. Some metals concentrations are nowadays sufficient to be taken into account for mining purposes—Au, Ag and Cu, for instance—while other elements of great added value (i.e., REE) are present but in concentrations below the earth's crust abundance [28,29]. On the other hand, it is important to note the high concentration of potential deleterious metals such as As (2.30 wt%), which highlights the importance of analyzing metals when tailings deposits are characterized. The high content of As may affect the potential treatment applied to the material to benefit any metal of interest. Treatments such as leaching would need to be very selective.

Small differences were found between the results obtained by different chemical analysis methods (XRF vs. ICP-OES). It is observed in Fe assays, 20.30 wt% vs. 25.26 wt%, or in S assays, 5.00 wt% vs. 12.76 wt%. For a more accurate sulfur determination, a Leco Sulphuur analyzer is recommended. However, other metals such as Cu and Zn correlated well, 0.29 wt% for Cu in both cases, and 0.19 wt% vs. 0.20 wt% for Zn. Greater differences are identified in minor elements (i.e., Ag, Co, . . .); this could be explained due to the fact that XRF analysis is semi-quantitative.

Mineralogical analysis presented serious challenges due to the physical–chemical effects of the sample. The origin of the material (roasted pyrite), weathering along the years and particle size were identified as the main causes for challenging mineralogical interpretation. Three samples were prepared for CAMEVA mineralogical examination, and issues during the preparation were reported due to fine grains (0.1–200 μm) found in the sample. Only one of the three samples (sample C) had sufficient quality to be examined. Furthermore, the examination reported sphalerite content (4.65 wt%); however, this content was not consistent with Zn concentrations reported in the XRF analysis. A second look was required, and it was found that sphalerite and minio (a Pb-bearing oxide mineral) had similar multispectral signatures; this finding correlated better with Pb content (2.08 wt%). Results from the CAMEVA system would be considered as inconclusive if no other techniques were applied during the study; however, the combination of different mineralogical techniques allowed a better interpretation. Mineralogical analysis using X-ray diffraction with Aeris overcame the limitations of microscopic techniques when analyzing fine-grained materials (D_{80} = 23 μm). It was beyond the scope of this paper to perform quantitative XRD analysis via the Rietveld method.

The presence of fine material in the tailings deposit was confirmed twice: first with SEM-EDS analysis and second with the use of a laser diffractometer. This fine particle size would be key for potential metallurgical separation/extraction technique selection.

One of the most interesting metals found during the characterization was copper. The copper content of the sample (0.29 wt%) is higher than the cut-off grade (0.16 wt%) reported by the nearby Riotinto mine in its latest NI 43-101 report (September 2022). However, the copper-bearing minerals might not be the same. The main copper mineral in Atalaya Mining is chalcopyrite (1.1 wt%) [21]. The mineralogical analysis (CAMEVA, XRD and SEM-EDS) carried out during the study did not show which minerals bear copper. This could be explained due to the fact that the tailings deposit hosts morrongos (residues from pyrite roasting processes). Additionally, a sequential copper test showed that 78.5% of copper was soluble and more than 90% could be considered as leachable, which would make a leaching treatment ideal for copper beneficiation. Moreover, the acidic natural pH reported (pH 2.0) would decrease the acid consumption in a hypothetical leaching process in acidic medium. Further investigation is required on this regard.

The first volume estimations were completed in 1999–2002 by MRT SAL [24,30], the second were completed in 2014 by EMED Mining, and finally, the last were completed in 2022 during the present study by the author. Although the estimation carried out by EMED Mining was completed in 2014, it must be noted that during 1999–2000, some mining

activities were reported in the deposit. A volume of 243,449 m^3 was mined due to its gold (1.40 g/t) and silver (94 g/t) content. Different techniques as well as software were used in order to estimate the volume present in the deposit.

The present study showed differences with the estimation completed in 2002, which were mainly in the volume, 824,612 m^3 vs. 638,425 m^3, and metal grades. Nevertheless, the copper (metal) content is in the same range, as the volume is lower in a case but higher in grade.

The gross estimation reserves demonstrated differences between analysis techniques; however, metals such as Cu or Ag were not very affected, although others such as Co or Sb decreased their presence significantly. For economic estimations, the most conservative figures were taken into account.

The presence and concentrations of secondary and critical raw materials might make this deposit attractive from an economic point of view. The deposit has a potential value of 19 million USD in copper and 1.47 millon USD in cobalt (LME average prices for December 2022) [31,32].

As seen in Figures 9 and 10, the deposit aging provides evidence. According to the IGME online tailings deposit database [18], this deposit represents a source of pollution to the Riotinto river and a source of dust in the surroundings. This situation might change if a process that benefits the secondary and/or critical raw materials present in the deposit is found.

5. Conclusions

The main conclusions of the present research are summarized:

1. Due to the chemical complexity of the sample, it is necessary to combine different analysis techniques for a correct characterization.
2. Mineralogical analyses indicate the presence of altered mineral phases, oxides and a low proportion of sulfides.
3. Several critical raw materials have been identified: As, Cu, Sb, Co, Bi, REE and PGM. Some of them have significant concentrations (Au, Ag).
4. Coarse size material is usually stored in waste dumps, while fine material is normally stored in tailing dams. The storage of this ultra-fine grain size material in a waste dump shape deposit is unusual. The fact of the ultra-fine size of the material might be one of the factors accelerating the aging of the deposit.
5. The chemical and physical properties of the sample, as well as the sequential leaching test, suggest that metallurgical techniques such as leaching or a combination of flotation and leaching might be a successful process for metal extraction.
6. The Zarandas deposit hosts approximately 824,612 m^3 of material. As it was estimated from a single small sample taken from a single spot, metals such as copper or cobalt account for 2358 t and 108 t, respectively. It means that the deposit has a potential value of 19 million USD in copper and 5.5 million USD in cobalt.

Author Contributions: Conceptualization, D.D. and A.M.; methodology, D.D.; software, D.D.; validation, D.D. and A.M.; formal analysis, D.D.; investigation, D.D.; resources, D.D. and A.M.; data curation, D.D.; writing—original draft preparation, D.D.; writing—review and editing, D.D. and A.M.; supervision, A.M.; funding acquisition, A.M. All authors have read and agreed to the published version of the manuscript.

Funding: This research has been funded by Ministerio de Ciencia, Innovación y Universidades (MCIU), Agencia Estatal de Investigación (AEI), and Fondo Europeo de Desarrollo Regional (FEDER) with grant number RTI2018-096695-B-C31.

Data Availability Statement: Data will be provided after request.

Acknowledgments: To Atalaya Riotinto Minera SLU, Fundación Riotinto, Malvern Panalytical, Emilio Romero, Jesús de la Rosa, José Miguel Nieto, Ignacio Silva, Aquilino Delgado, Úrsula Grundwald, Juan Carlos Catalina, Ricardo Castro Viejo, María Maestre, David Menéndez, Elisa Arenas, Matteo Pernechele and specially to José Manuel Fidalgo for the guidance and support all along the process.

Conflicts of Interest: The authors declare no conflict of interest. The funders had no role in the design of the study; in the collection, analyses, or interpretation of data; in the writing of the manuscript; or in the decision to publish the results.

References

1. Grohol, M.; Veeh, C.; Grow, D.G. European Commission. In *European Commission, Study on the Critical Raw Materials for the EU 2023–Final Report*; Publication Office of the European Union: Brussels, Belgium, 2023. [CrossRef]
2. Northey, S.; Mohr, S.; Mudd, G.M.; Weng, Z.; Giurco, D. Modelling future copper ore grade decline based on a detailed assessment of copper resources and mining. *Resour. Conserv. Recycl.* **2014**, *83*, 190–201. [CrossRef]
3. United Nations. *Report of the World Commission on Environment and Development: Our Common Future; General Assembly Resolution 42/187*; United Nations: Rio de Janeiro, Brazil; New York, NY, USA, 1987.
4. Li, H.; Oraby, E.; Eksteen, J.; Mali, T. Extraction of Gold and Copper from Flotation Tailings Using Glycine-Ammonia Solutions in the Presence of Permanganate. *Minerals* **2022**, *12*, 612. [CrossRef]
5. Marín, O.A.; Kraslawski, A.; Cisternas, L.A. Estimating processing cost for the recovery of valuable elements from mine tailings using dimensional analysis. *Miner. Eng.* **2022**, *184*, 107629. [CrossRef]
6. Araya, N.; Kraslawski, A.; Cisternas, L.A. Towards mine tailings valorization: Recovery of critical materials from Chilean mine tailings. *J. Clean. Prod.* **2020**, *263*, 121555. [CrossRef]
7. Sarker, S.K.; Haque, N.; Bhuiyan, M.; Bruckard, W.; Pramanik, B.K. Recovery of strategically important critical minerals from mine tailings. *J. Environ. Chem. Eng.* **2020**, *10*, 107622. [CrossRef]
8. Vara, P. *Pirita de Huelva: Su historia, Minería y Aprovechamiento*; Consulcom: Huelva, Spain, 1963; pp. 172–175.
9. López-Arce, P.; Garrido, F.; García-Guinea, J.; Voegelin, A.; Göttlicher, J.; Nieto, J.M. Historical roasting of thallium–and arsenic–bearing pyrite: Current Tl pollution in the Riotinto mine area. *Sci. Total Environ.* **2019**, *648*, 1263–1274. [CrossRef] [PubMed]
10. Durán García, F. *Proceso Industrial de la Planta Lavadora de Naya de la R.T.C.L*; Minas de Riotinto: Huelva, Spain.
11. Romero, A.; González, I.; Galán, E. Estimation of potential pollution of waste mining dumps at Peña del Hierro (Pyrite Belt, SW Spain) as a base for future mitigation actions. *Appl. Geochem.* **2006**, *21*, 1093–1108. [CrossRef]
12. Ortiz Mateo, M.; Romero, E. Aproximación a la minería y Metalurgia de Minas de Riotinto desde la antigüedad al siglo XIX. Ph.D. Thesis, Escuela Técnica Superior de Ingenieros de Minas y Energía, Madrid, Spain, 2003; 632p. [CrossRef]
13. Arranz González, J.C.; Cala Rivero, V. Evaluación de la movilidad de metales pesados en residuos mineros de flotación de minería metálica en la provincia de Huelva. *Bol. Geol. Min.* **2011**, *22*, 203–220.
14. Arranz González, J.C.; Cala Romero, V.; Iribarren Campaña, I. Geochemistry and mineralogy of surface pyritic tailings impoundments at two mining sites of the Iberian Pyrite Belt (SW Spain). *Env. Earth Sci* **2012**, *65*, 669–680. [CrossRef]
15. Arranz González, J.C.; Rodríguez-Gómez, V.; Fernández-Naranjo, F.J.; Vadillo-Fernández, L. Assessment of the pollution potential of a special case of abandoned sulfide tailings impoundment in Riotinto mining district (SW Spain). *Environ. Sci. Pollut. Res.* **2012**, *28*, 14054–14067. [CrossRef] [PubMed]
16. Pérez-López, R.; Sáez, R.; Álvarez-Valero, A.M.; Nieto, J.M.; Pace, G. Combination of sequential chemical extraction and modelling of dam-break wave propagation to aid assessment of risk related to the possible collapse of a roasted sulphide tailings dam. *Sci. Total Environ.* **2009**, *407*, 5761–5771. [CrossRef] [PubMed]
17. Ruiz Cánovas, C.; Moreno González, R.; Vieira, B.J.C.; Waerenborh, J.C.; Marques, R.; Macías, F.; Basallote, M.D.; Olias, M.; Prudencio, M.I. Metal mobility and bioaccessibility from cyanide leaching heaps in a historical mine site. *J. Hazard. Mater.* **2023**, *448*, 130948. [CrossRef] [PubMed]
18. CN IGME (2022/2001). IGME Balsas–InfoIGME ©CN Instituto Geológico y Minero de España. Available online: http://info.igme.es/balsas//0938-8-0002 (accessed on 20 December 2022).
19. Catalina, J.C.; Castroviejo, R. Microscopía de reflectancia multiespectral: Aplicación al reconocimiento automatizado de menas metálicas. *Rev. Metal.* **2017**, *53*, e107. [CrossRef]
20. López-Benito, A.; Catalina, J.C.; Alarcón, D.; Grunwald, Ú.; Romero, P.; Castroviejo, R. Automated ore microscopy based on multispectral measurements of specular reflectance. I–A comparative study of some supervised classification techniques. *Miner. Eng.* **2020**, *146*, 106136. [CrossRef]
21. Pernechele, M.; López, Á.; Davoise, D.; Maestre, M.; König, U.; Norberg, N. Value of Rapid Mineralogical Monitoring of Copper Ores. *Minerals* **2021**, *11*, 1142. [CrossRef]
22. Han, N.K.; Doyle, F.; Arbiter, N. *Mineral Processing and Extractive Metallurgy Review*; Gordon and Breach Science Publishers: Philadelphia, PA, USA, 1991; Volume 7, pp. 175–207.
23. METCON Research Inc. *Sequential Copper Analysis: Acid Soluble Copper, Cyanide Soluble Copper and Residual Copper*; METCON Research Inc.: Pembroke, NC, USA, 2001; p. 2.

24. MRT S.A.L. *Zarandas II. Informe Geológico y Estimación de Reservas*; MRT S.A.L.: Minas de Riotinto, Spain, 1999; p. 62.
25. Centro de Descargas. Organismo Autónomo Centro Nacional de Información Geográfica. Available online: http://centrodedescargas.cnig.es/CentroDescargas/catalogo.do?Serie=PNOIR# (accessed on 20 December 2022).
26. Instituto Geográfico Nacional Especificaciones Técnicas Vuelo de Segunda Cobertura. Available online: https://pnoa.ign.es/web/portal/pnoa-lidar/especificaciones-tecnicas (accessed on 20 December 2022).
27. EMED. *Mining A report on Zarandas II Resource*; EMED: Minas de Riotinto, Spain, 2014; p. 6.
28. Balaram, V. Rare earth elements: A review of applications, occurrence, exploration, analysis, recycling, and environmental impact. *Di Xue Qian Yuan* **2019**, *10*, 1285–1303. [CrossRef]
29. Kumari, A.; Panda, R.; Jha, M.K.; Kumar, J.R.; Lee, J.Y. Process development to recover rare earth metals from monazite mineral: A review. *Miner. Eng.* **2015**, *79*, 102–115. [CrossRef]
30. MRT, S.A.L. *Extraído de Zarandas II*; MRT S.A.L.: Minas de Riotinto, Spain, 2002; p. 1.
31. London Metal Exchange, LME Copper. Available online: https://www.lme.com/en/Metals/Non-ferrous/LME-Copper#Trading+day+summary (accessed on 1 January 2023).
32. London Metal Exchange, LME Cobalt. Available online: https://www.lme.com/en/Metals/EV/LME-Cobalt#Trading+day+summary (accessed on 1 January 2023).